Vibrational Spectra and Isotope Effect of Dihydroxylammonium 5，5'-Bis(Tetrazole)-1，1'-Diolate under High Pressure

ZHAO Sheng-xiang[1]，SONG Xue-yan[2]，XING Xiao-ling[1]，LI Yan[2]，JU Xue-hai[2]*

1. Xi'an Modern Chemistry Research Institute，Xi'an 710065，China
2. School of Chemical Engineering，Nanjing University of Science and Technology，Nanjing 210094，China

Abstract Density functional theory calculations were performed on crystalline dihydroxylammonium 5，5'-bis (tetrazole)-1，1'-diolate (HATO) under high pressure up to 40 GPa. The GGA-PW91 method in combination with the ultrasoft pseudopotentials reproduced the experimental crystal structure of HATO and was thus employed for the optimizations of both molecular structure and cell parameters. The intermolecular O…H distances generally decrease with increasing pressures. However，the O—H and N—H bond lengths change irregularly upon pressure. Based on the optimized crystal structures at different pressures，the non-periodic calculations of frequencies with a scaling factor of 0.967 9 were used to predict both the IR and Raman spectra. The predicted strongest Raman peak at 1 580 cm^{-1}，involving C—C stretching and NH_2 symmetric deformation，is in agreement with the experiment. Although there is no hydrogen atom in the anion moiety of HATO，the deuteration in cation still affects the vibrational mode of anion. For O—H and O—D vibration modes，the Raman shifts decrease due to the strengthening intermolecular hydrogen bond as the pressure increases. Upon deuteration，the most characterized change of Raman shifts for ND_2 is that the ν_2 stretching mode increases dramatically with high pressure as compared to those of NH_2，which leads to a coupling of ND_2 ν_2/ν_3 modes at high pressure. The calculated isotopic ratios，$\nu(NH_2)/\nu(ND_2)$ for ν_1 to ν_3 modes，are in the range of 1.36～1.38，which are in consistent with the value from the reduced masses of these atoms. The couplings of vibrational modes change with both deuteration and pressure.

Keywords Dihydroxylammonium 5，5'-bis(tetrazole)-1，1'-diolate (HATO)；IR and Raman；High pressure；H/D Isotope effect；Density functional theory

中图分类号：O657.6 **文献标识码**：A **DOI**：10.3964/j.issn.1000-0593(2019)09-2946-07

Introduction

An increasing attention has been paid to energetic salts in recent years since their overall properties could be optimized by the chemical modification of both ions[1-4]. The coulomb interaction between anions and cations makes them have high density and stability compared with their atomically similar nonionic analogues. Niko Fischer et al. synthesized an energetic salts of dihydroxylammonium 5，5'-bistetrazole-1，1'-diolate (HATO). They found that it has a detonation velocity comparable to 2，4，6，8，10，12-hexanitro-2，4，6，8，10，12-hexaazatetracyclo[5.5.0.0.0]dodecane (CL-20) but lower sensitivity than commonly used high energy explosives such as cyclotetramethylene tetranitramine (HMX) and CL-20，indicating that HATO could be used as a promising insensitive high energetic material[5-7]. To probe insight into its microscopic factors of its low sensitivity，some investigations have been conducted to characterize the behaviors under high pressure and high temperature by theoretical as well as experimen-

Received：2018-06-15；**accepted**：2018-12-12

Foundation item：National Natural Science Foundation of China (21207066)

Biography：ZHAO Sheng-xiang，(1963—)，research fellow，Xi'an Modern Chemistry Research Institute

* Corresponding author e-mail：xhju@njust.edu.cn

tal methods. Dreger et al. used Raman spectroscopy to probe the stability of HATO and found that it transforms to two consecutive intermediates in heating[8]. An et al. studied the atomistic reaction mechanisms for the initial thermal decompositions of this system at high temperature by the quantum mechanics. They found that the protonated or deprotonated bistetrazole in the periodic system decompose under continuous heating, which eventually leads to the release of N_2 and N_2O[9]. The ionic energetic compounds are chemically stable over a broad range of pressure in comparison with their neutral analogues due to the strong Coulomb attraction between the counter ions, and some changes of the Coulomb attraction will take place at high pressure. It is reasonable to associate the shock initiation with the changes of interionic forces. The variations of vibrational spectra of HATO under high pressures as well as the deuteration effects were probed.

1　Computational details

The crystal structure obtained from the X-ray diffraction was used as the initial structure for the bulk (CCDC 872232). The unit cell of HATO was found to be $a=0.544\ 1$, $b=1.175\ 1$, $c=0.656\ 1$ nm and $\beta=95.07°$[5], crystallizing in space group P21/c (Fig. 1). There were two irreducible anions and four cations in the unit cell. The generalized gradient approximation (GGA) method at the Perdew-Burke-Ernzerhof (PBE) and Perdew-Wang (PW91) levels and the ultrasoft psudopotentials were employed for the optimizations of cell parameters and molecular geometries, with dispersion force correction. Although the method includes the electron correlation, it is still computationally economic. The threshold for energy convergence is 2×10^{-6} eV/atom in optimizing. The optimizations were performed with CASTEP code[10]. The optimized cell parameters are $a=0.501\ 3$, $b=1.333\ 9$, $c=0.724\ 7$ nm and $\beta=100.00°$ at the GGA-PBE level, and $a=0.543\ 5$, $b=1.224\ 6$, $c=0.682\ 5$ nm and $\beta=95.77°$ at the GGA-PW91 level. Therefore, the latter method is better and more suitable for HATO crystal. Consequently, all the geometrical optimizations for the crystal at high pressures were performed by the GGA-PW91 method. Since the deuteration does not change the electronic structure of the ions, the geometrical structures before and after the deuteration are identical. Then the vibrational frequencies were obtained by a single point calculation on the structures of ionic pairs from the optimized cell at high pressures. The non-periodic calculation of frequency was performed by the density functional theory method of Becke3-Lee-Yang-Parr (B3LYP) that produces consistent results with experiment[11-13]. The Gaussian 09 procedure was employed for the frequency calculations[14]. A scaling factor of 0.967 9 was adopted for the correction of frequencies[15].

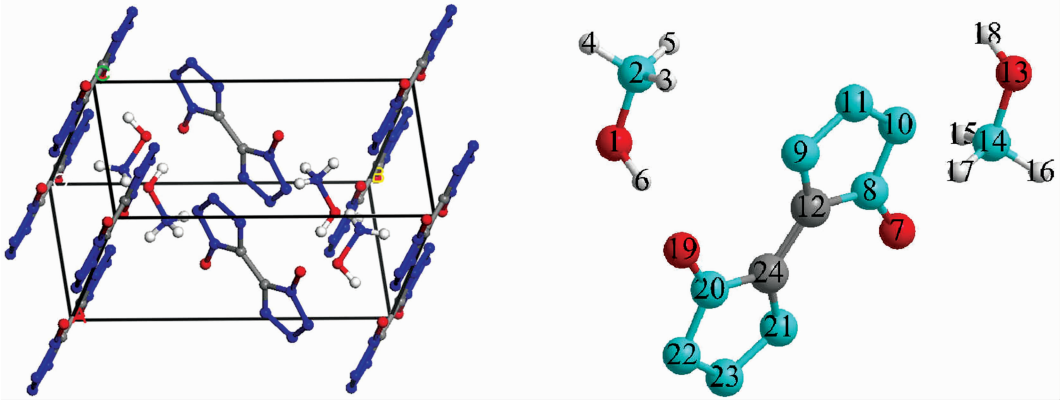

Fig. 1　Crystal structure and atomic numbering of dihydroxylammonium 5,5'-bis(tetrazole)-1,1'-diolate
(Oxygen in red, nitrogen in blue or green, carbon in grey and hydrogen in light grey)

2　Results and discussion

2.1　Optimized crystal and molecular parameters

The optimized cell parameters at the GGA-PW91 level were listed in Table 1. The optimized cell parameters at both 0.0 and 0.1 GPa are consistent with the experimental values. On going from 0.0 to 40 GPa, the cell parameters of a, b and c decrease by 2.3%, 23.3% and 14.9%, respectively, indicating that the crystal is easily compressible along b and c axes compared to a axis. The pressure on a axis leads to two anions approaching with each other, thus a axis is less compressible. The crystal lattice energy is $-1\ 015.71$ kJ·mol^{-1} after corrected by dispersion forces. This large lattice energy is favorable for the stability of HATO and makes some contributions to its low sensitivity in response to mechanical stimulus. As can be seen from Table 2, the intermolecular distances change more than those of bond lengths. The intermo-

lecular O⋯H distances generally decrease with increasing pressures, especially for the NO⋯HN distances. The C—C bond lengths slightly decrease with increasing pressures. However, the O—H and N—H bond lengths changes irregularly upon pressures. When the repulsion between these two atoms becomes too large upon pressure, the N—O internal rotation will occur to avoid an accumulated repulsion within O—H and N—H bonds. The variations of intermolecular distances and bond lengths bring about the shifts of vibrational frequencies as discussed below.

Table 1 Optimized crystal structures of dihydroxylammonium 5,5'-bis(tetrazole)-1,1'-diolate under pressures

Pressure	*a*	*b*	*c*	*β*	*V*
0.0	5.435	12.246	6.583	95.77	435.94
0.1	5.443	12.181	6.585	95.98	434.20
10.0	5.439	10.484	6.110	98.27	344.77
20.0	5.379	9.862	5.916	99.48	309.51
30.0	5.321	9.565	5.761	100.97	287.85
40.0	5.307	9.388	5.600	103.35	271.47
Expt.	5.441	11.751	6.561	95.07	417.86

Pressure in GPa; *a*, *b* and *c* in Angstrom; *β* in degree; *V* in Å^3.

Table 2 Some bond and hydrogen bond lengths of dihydroxylammonium 5,5'-bis(tetrazole)-1,1'-diolate under pressures

Pressure	NO⋯HO	NO⋯HN	C—C	O—H	N—H
0.0	1.594	1.820	1.429	1.027	1.059
0.1	1.599	1.810	1.428	1.026	1.060
10.0	1.472	1.682	1.413	1.034	1.053
20.0	1.445	1.630	1.400	1.032	1.040
30.0	1.420	1.561	1.392	1.031	1.047
40.0	1.437	1.542	1.384	1.027	1.029

Pressure in GPa; Atomic distance in Angstrom.

2.2 Vibrational assigns at ambient pressure

The overall IR and Raman spectra of HATO at standard pressure are shown in Fig. 2 and those of its deuterated analogue are shown in Fig. 3. Fifteen IR frequencies with large adsorption intensities before and after deuterium substituting at standard atmospheric pressure are listed in Table 3 and Table 4, respectively. The O1-H6 stretching of hydroxyl exhibits a very intense peak at 2 486 cm^{-1} which shifts to 1 841 cm^{-1} by deuterium substituting. The next intense peak at 2 616 cm^{-1} is assigned to symmetric deformation of protonated amino, which shifts to 1 931 cm^{-1} by deuterium substituting (deuteration). These large shifts of frequencies after deuterium substitution are mainly due to the great change of the reduced mass in deuteration. Classically, vibrational frequency for two atoms is inversely proportional to the root square of the corresponding reduced mass. Moreover, the shifts of frequencies lead to the changes of vibrational coupling.

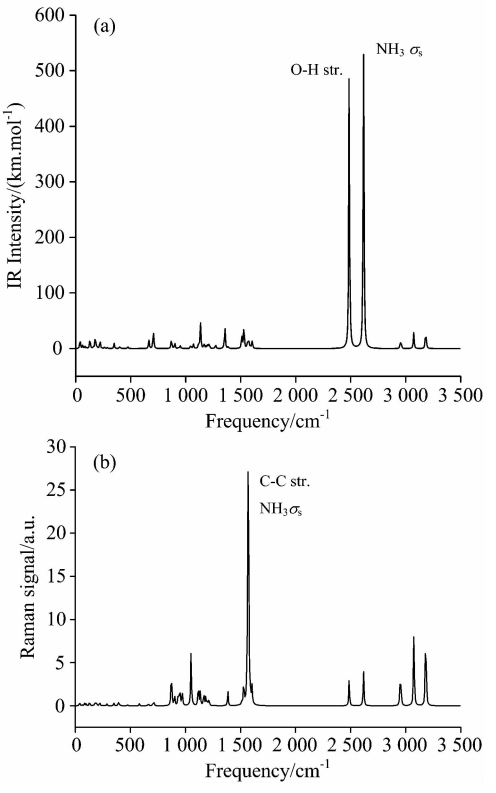

Fig. 2 IR and Raman spectra of dihydroxylammonium 5,5'-bis(tetrazole)-1,1'-diolate at standard pressure

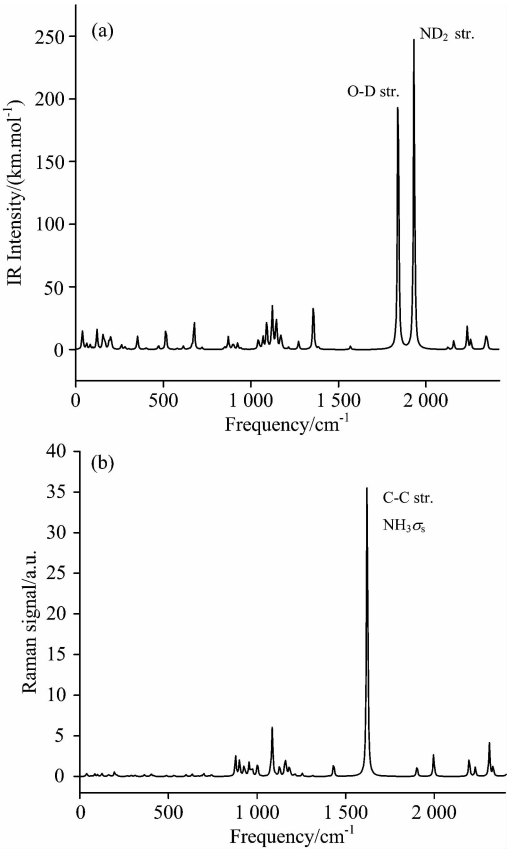

Fig. 3 IR and Raman spectra of deuterated dihydroxylammonium 5,5'-bis(tetrazole)-1,1'-diolate at standard pressure

Table 3　Vibrational modes, frequency and IR intensity of dihydroxylammonium 5,5'-bis(tetrazole)-1,1'-diolate

No.	Frequency	IR Intensity	Vibrational Modes
ν_1	3 186.32	16.19	H_{15}-N_{14}-H_{16} str.
ν_2	3 178.68	13.98	H_3-N_2-H_4 str.
ν_3	3 074.52	13.76	H_{15}-N_{14}-H_{16} str.
ν_4	3 071.47	16.09	H_3-N_2-H_4 str.
ν_5	2 957.37	12.27	O_{13}-H_{18} str.
ν_6	2 616.68	529.63	H_{15}-N_{14}-H_{16}-H_{17} σ_s
ν_7	2 486.12	471.40	O_1-H_6 str.
ν_8	1 529.30	32.24	H_3-N_2-H_4 sci., O_1-H_6 r.
ν_9	1 525.78	10.00	H_{15}-N_{14}-H_{16}-H_{17} σ_s, O_{13}-H_{18} r.
ν_{10}	1 509.70	23.20	H_3-N_2-H_4-H_5 σ_s, O_1-H_6 r.
ν_{11}	1 356.02	40.24	C_{12}-N_8 str., C_{24}-N_{20} str.
ν_{12}	1 134.40	41.36	ring breathing
ν_{13}	900.99	10.07	N_{10}-N_{11} str., N_{22}-N_{23} str.
ν_{14}	867.98	10.95	O_1-H_6 r.
ν_{15}	705.38	26.75	O_{13}-H_{18} r.

Frequency in cm^{-1}. Abbreviation used: str, stretching; r, rocking; sci, scissoring; σ_s, symmetric deformation; σ_{as}, asymmetric deformation.

Table 4　Vibrational modes, frequency and IR intensity of deuterated dihydroxylammonium 5,5'-bis(tetrazole)-1,1'-diolate

No.	Frequency	IR Intensity	Vibrational Modes
ν_1	2 348.89	8.18	D_{15}-N_{14}-D_{16} str.
ν_2	2 341.04	8.19	D_3-N_2-D_4 str.
ν_3	2 235.80	16.53	D_{15}-N_{14}-D_{16} str.
ν_4	1 931.92	236.64	D_{15}-N_{14}-D_{16} str., N_{14}-D_{17} str.
ν_5	1 841.09	223.76	O_1-D_6 str.
ν_6	1 357.05	37.16	C_{12}-N_8 str., C_{24}-N_{20} str.
ν_7	1 169.16	9.32	D_4-N_2-D_5 sci.
ν_8	1 145.81	11.47	D_{15}-N_{14}-D_{17} r., D_3-N_2-D_5 r., O_{13}-D_{18} r.
ν_9	1 123.00	19.86	D_3-N_2-D_4 sci.
ν_{10}	1 120.57	12.65	D_{15}-N_{14}-D_{16}-D_{17} σ_{as}, ring breathing
ν_{11}	1 090.83	22.93	D_4-N_2-D_5 sci., O_1-D_6 r.
ν_{12}	1 069.23	8.60	N_{10}-N_{11} str., N_{22}-N_{23} str.
ν_{13}	1 042.54	7.91	ring deformation
ν_{14}	870.83	7.99	N_{14}-D_{15}-D_{16}-D_{17} σ_s
ν_{15}	676.27	21.07	ring breathing, O_1-D_6 r.

Frequency in cm^{-1}. Abbreviation used: str, stretching; r, rocking; sci, scissoring; σ_s, symmetric deformation; σ_{as}, asymmetric deformation

Frequencies in the range of 2 957 to 3 186 cm^{-1} belong to the O—H and N—H stretching of hydroxylammonium cation. There are weak peaks at 705 and 867 cm^{-1} for O—H rocking, which shift to 676 cm^{-1} by deuteration. As can be seen in Fig. 2 and Fig. 3, vibrational modes of H/D substitution at three highest frequencies are identical, while some low frequencies belong to different modes. Compared to HATO, one obvious difference in IR spectra after deuteration is that there exist weak peaks at 1 120～1 170 cm^{-1} for D-N-D scissoring/rocking or O-D rocking or ring breathing. The IR frequency of N-N stretching blueshifts from 900 to 1 069 cm^{-1} upon deuteration. Although these is no hydrogen atom in the anion moiety of HATO, the deuteration in cation still affects the vibrational mode of anion. The Raman spectra of HATO (Fig. 2) and its deuterated analogues (Fig. 3) look similar except for frequency decreasing upon deuteration.

2.3　Isotopic effects on Raman spectra

As can be seen in Fig. 4, the Raman spectra in the range of 800 to 1 600 cm^{-1} are generally similar as a whole with only one exception that there are two weak peaks on the opposite side of the strongest peak at 1 580 cm^{-1} for NH_2 scissoring of HATO. However, these two peaks disappear upon deuteration. It is worthy to note that the strongest peak at 1 580 cm^{-1} is in good agreement with the experiment[8], indicating the computational method is suitable to the title compound. As can be seen in left amplified figures, a weak peak at 160 cm^{-1} increases its intensity, and a double peak at 180～190 cm^{-1} emerges into one peak with intensity decreasing upon deuteration. The vibrational modes of NH_2 stretching ν_1/ν_2 at 3 180 cm^{-1} red shift upon deuteration, and ν_3/ν_4 at 3 090 cm^{-1} of HATO also red shift and at the same time split into two peaks upon deuteration. The calculated isotopic ratio,

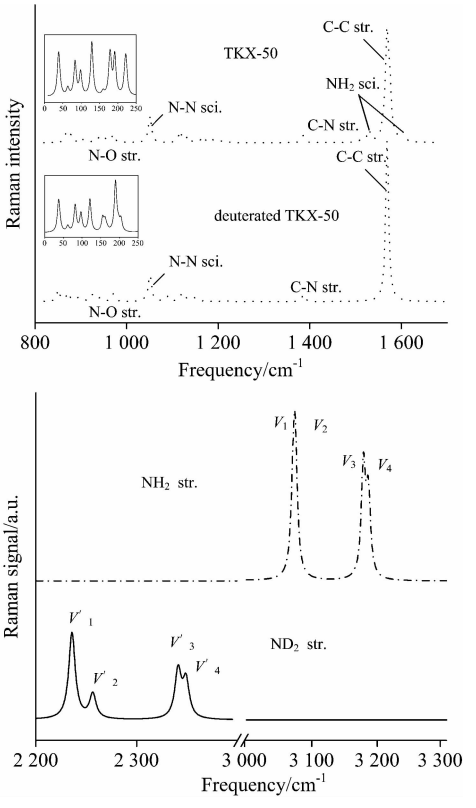

Fig. 4　Isotopic effect on Raman spectra of dihydroxylammonium 5,5'-bis(tetrazole)-1,1'-diolate (HATO)

$\nu(NH_2)/\nu(ND_2)$ for ν_1 to ν_3 modes are in the range of 1.36～1.38, which are consistent with the value of 1.39 obtained from the ratios of reduced masses for these atoms. However, $\nu(NH_2)/\nu(ND_2)$ for ν_4 mode is as large as 1.59 since the $\nu_4(NH_2)$ and $\nu_4(ND_2)$ modes are not identical with modes coupling involved in the latter.

2.4 Spectra at high pressures

Fig. 5 displays the Raman spectra in pressure. In general, almost all the peaks blueshift as the pressure increase. The atomic equilibrium distances decrease when high pressure is imposed. This leads to the strengthening of chemical bonds as compared to those under standard pressure. However, the blueshift becomes smaller and smaller when the pressure comes up to 40 GPa since the nuclear repulsion between neighbor atoms increases dramatically as their distance decreases, i.e., the compressibility of chemical bonds become smaller. The Raman shifts vs. pressure is shown in Fig. 6. The Raman shifts for C—C stretching increase as the pressure increases. For two NH_3, σ deformations, one shift increases and another hardly change with increasing pressure. However, both the ND_3, σ deformations hardly change with increasing pressure. For O—H and O—D vibration modes, the Raman shifts decrease as the pressure increases. The intermolecular hydrogen bond O_{19}-H_6 increases as the pressure increases. Consequently, the O_1-H_6 bond weakens with increasing pressure. Fig. 7 shows the Raman shifts of the NH_2 and ND_2 stretching modes ν_1 to ν_4 under pressure. The Raman shifts of the ν_1 and ν_2 modes for NH_2 increase slightly with pressure increasing up to 20 GPa, but increase greatly over 30 GPa. The Raman shift of ν_3 mode increases but that of ν_4 mode decreases as a whole, leading to the $\nu_1/\nu_2/\nu_4$ modes coupling at high pressure as indicated by the oval circle in Fig. 7. Upon deuteration, the most characterized change of Raman shifts for ND_2 is that the ν_2 stretching mode increases dramatically with high pressure as compared to those of NH_2, which leads to a ND_2 ν_2/ν_3 modes coupling at high pressure.

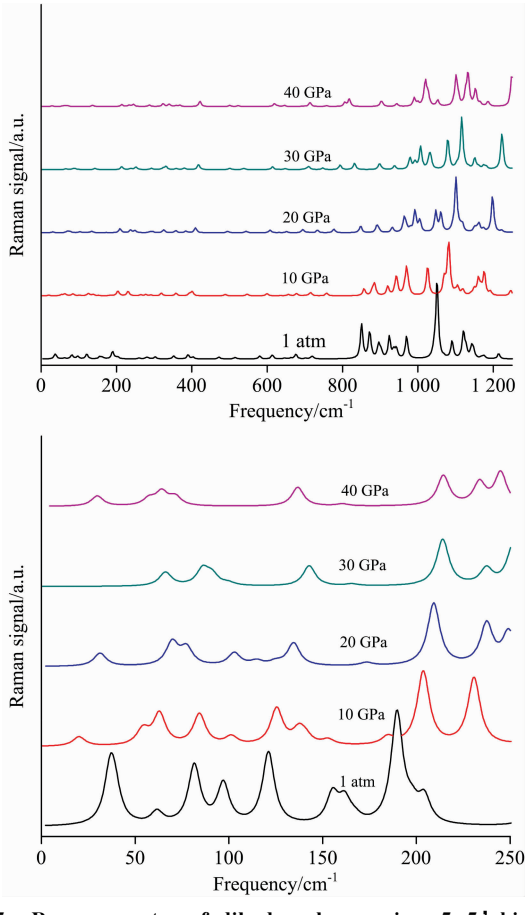

Fig. 5 Raman spectra of dihydroxylammonium 5,5'-bis(tetrazole)-1,1'-diolate on pressures

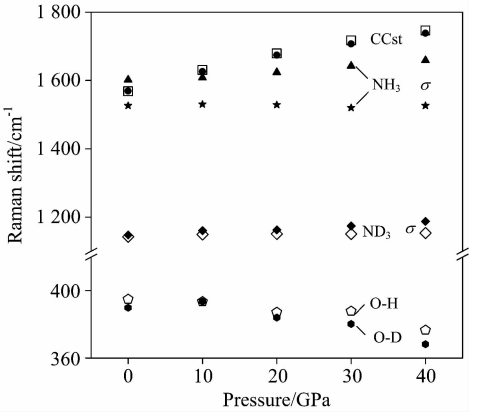

Fig. 6 Raman shifts vs. pressure of dihydroxylammonium 5,5'-bis(tetrazole)-1,1'-diolate

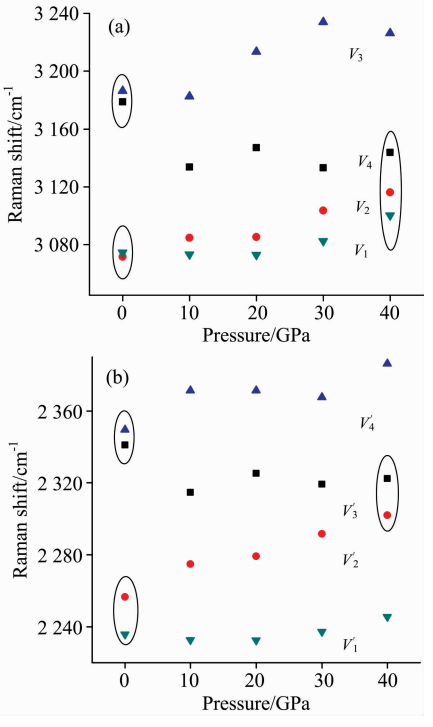

Fig. 7 Raman shifts of NH_2 str. (a) and ND_2 str. (b) *vs.* pressure (Oval circles indicate vibrational coupling between different modes)

3 Conclusions

The periodic density functional theory calculation together with ultrasoft psudopotentials reproduced the experimental crystal structure of HATO and was thus employed for the optimizations of both molecular structure and cell parameters. Based on the optimized crystal structure of HATO under high pressures up to 40 GPa and the non-periodic calculations of frequencies with a scaling factor of 0.967 9, the IR and Raman spectra at different pressures were predicted. The intermolecular O…H distances generally decrease with increasing pressures. However, the O—H and N—H bond lengths changes irregularly upon pressures. The predicted strongest Raman peak at 1 580 cm^{-1} involving C—C stretching and NH_2 symmetric deformation is in good agreement with the experiment, indicating the method is suitable for the title system. Although there is no hydrogen atom in the anion moiety of HATO, the deuteration in cation still affects the vibrational mode of anion. For O—H and O—D vibration modes, the Raman shifts decrease due to the strengthening intermolecular hydrogen bond as the pressure increases. The calculated isotopic ratio, $\nu(NH_2)/\nu(ND_2)$ for ν_1 to ν_3 modes are in the range of 1.36～1.38, which are in consistent with the value from the ratios of reduced masses for these atoms. The couplings of vibrational modes change with both deuteration and pressure. The results provided valuable information for understanding the properties of high energetic materials under high pressure.

References

[1] Meng Z Y, Zhao F Q, Xu S Y, et al. Canadian Journal of Chemistry, 2017, 95: 691.
[2] Xu Z, Cheng G B, Yang H W, et al. Angewandte Chemie International Edition, 2017, 56(21): 5877.
[3] Gao H, Shreeve J M. Chemical Review, 2011, 111(11): 7377.
[4] Xu S Y, Meng Z Y, Zhao F Q, et al. Canadian Journal of Chemistry, 2018, doi: 10.1139/cjc-2018-0106.
[5] Fischer N, Fischer D, Klapötke T M, et al. Journal of Materials Chemistry, 2012, 22: 20418.
[6] Fischer N, Klapötke T M, Reymann M, et al. European Journal of Inorganic Chemistry, 2013, 2167.
[7] Shang Y, Jin B, Liu Q, et al. Journal of Molecular Structure, 2017, 1133: 519.
[8] Dreger Z A, Breshike C J, Gupta Y M. Chemical Physics Letters, 2017, 679: 212.
[9] An Q, Liu W, William A G, et al. Journal Physical Chemistry C, 2014, 118: 27175.
[10] Clark S J, Segall M D, Pickard C J, et al. Zeitschrift für Kristallographie, 2005, 220: 567.
[11] Seminario J M, Politzer P. Modern Density Functional Theory: A Tool for Chemistry, Elsevier: Amsterdam, 1995.
[12] Zhu Gonghai, Chen Guoqing, Zhu Chun, et al. Spectroscopy and Spectral Analysis, 2018, 38(4): 1133.
[13] Çirak Ç, Körozlü N, Sert Y, et al. Spectroscopy and Spectral Analysis, 2018, 38(4): 1276.
[14] Frisch M J, Trucks G W, Schlegel H B, et al. Gaussian 09, Revision A.02, Gaussian, Inc., Wallingford CT, 2009.
[15] Andersson M P, Uvdal P. Journal Physical Chemistry A, 2005, 109(12): 2937.

高压下 1,1'-二羟基-5,5'-联四唑二羟胺盐的振动光谱及同位素效应

赵省向[1]，宋雪燕[2]，邢晓玲[1]，李　燕[2]，居学海[2*]

1. 西安近代化学研究所，陕西 西安　710065
2. 南京理工大学化工学院，江苏 南京　210094

摘　要　用密度泛函理论方法研究 1,1'-二羟基-5,5'-联四唑二羟胺盐(HATO)晶体在高压(＜40 GPa)下性质。在 GGA-PW91 计算水平并结合超软势基组对 HATO 晶体结构进优化，其优化结构能再现实验结果。分子间 O…H 间距随压力的增加而显著减小；但 O—H 和 N—H 键长呈现非单调变化。基于不同压力下的优化晶体结构，利用非周期性计算并经校正因子 0.967 9 校正，求得相应压力下的红外和拉曼谱。预测最强拉曼峰对应于 C—C 伸缩和 NH_2 对称变形，位于 1 580 cm^{-1}，与实验结果一致。虽然阴离子不含氢原子，但阳离子的氘代仍对阴离子的振动光谱产生影响。高压导致分子间氢键增强，导致参与氢键的 O—H 和 O—D 振动的拉曼波数减小。氘代后，ND_2 的拉曼位移的最明显变化是 ν_2 伸缩振动波数在高压下急剧增加，导致 ND_2 ν_2/ν_3 在高压下发生偶合。计算出的 ν_1 至 ν_3 振动的同位素效应比 $\nu(NH_2)/\nu(ND_2)$ 均为 1.36～1.38，与由折

合质量所求得的值相一致。氘代和压力的变化可引起不同振动模式的偶合。

关键词 5,5'-联四唑-1,1'-二氧二羟铵(TKX-50)；红外和拉曼光谱；高压；H/D 同位素效应；密度泛函理论

(收稿日期：2018-06-15，修订日期：2018-12-12)

* 通讯联系人